remote sensing

MDPI

Article

Decomposing the Long-term Variation in Population Exposure to Outdoor $PM_{2.5}$ in the Greater Bay Area of China Using Satellite Observations

Changqing Lin [1,2], Alexis K. H. Lau [1,2,*], Jimmy C. H. Fung [1,3], Qianshan He [4], Jun Ma [2], Xingcheng Lu [1], Zhiyuan Li [1], Chengcai Li [5], Renguang Zuo [6] and Andromeda H. S. Wong [1]

1 Division of Environment and Sustainability, the Hong Kong University of Science and Technology, Hong Kong, China; cqlin@ust.hk (C.L.); majfung@ust.hk (J.C.H.F.); xclu@ust.hk (X.L.); zliar@connect.ust.hk (Z.L.); ahswongaa@ust.hk (A.H.S.W.)
2 Department of Civil and Environmental Engineering, the Hong Kong University of Science and Technology, Hong Kong, China; jackma@ust.hk
3 Department of Mathematics, the Hong Kong University of Science and Technology, Hong Kong, China
4 Shanghai Meteorological Service, Shanghai 200030, China; oxeye75@163.com
5 Department of Atmospheric and Oceanic Sciences, School of Physics, Peking University, Beijing 100871, China; ccli@pku.edu.cn
6 State Key Laboratory of Geological Processes and Mineral Resources, China University of Geosciences, Wuhan 430074, China; zrguang@cug.edu.cn
* Correspondence: alau@ust.hk; Tel.: (852)-2358-6676

Received: 16 October 2019; Accepted: 11 November 2019; Published: 13 November 2019

Abstract: The Greater Bay Area (GBA) of China is experiencing a high level of exposure to outdoor $PM_{2.5}$ pollution. The variations in the exposure level are determined by spatiotemporal variations in the $PM_{2.5}$ concentration and population. To better guide public policies that aim to reduce the population exposure level, it is essential to explicitly decompose and assess the impacts of different factors. This study took advantage of high-resolution satellite observations to characterize the long-term variations in population exposure to outdoor $PM_{2.5}$ for cities in the GBA region during the three most-recent Five-Year Plan (FYP) periods (2001–2015). A new decomposition method was then used to assess the impact of $PM_{2.5}$ variations and demographic changes on the exposure variation. Within the decomposition framework, an index of pollution-population-coincidence–induced $PM_{2.5}$ exposure (PPCE) was introduced to characterize the interaction of $PM_{2.5}$ and the population distribution. The results showed that the 15-year average PPCE levels in all cities were positive (e.g., 6 $\mu g/m^3$ in Guangzhou), suggesting that unfavorable city planning had led to people dwelling in polluted areas. An analyses of the spatial differences in $PM_{2.5}$ changes showed that urban areas experienced a greater decrease in $PM_{2.5}$ concentration than did rural areas in most cities during the 11th (2006–2010) and 12th (2011–2015) FYP periods. These spatial differences in $PM_{2.5}$ changes reduced the PPCE levels of these cities and thus reduced the exposure levels (by as much as -0.58 $\mu g/m^3$/year). The population migration resulting from rapid urbanization, however, increased the PPCE and exposure levels (by as much as 0.18 $\mu g/m^3$/year) in most cities during the three FYP periods considered. Dongguan was a special case in that the demographic change reduced the exposure level because of its rapid development of residential areas in cleaner regions adjacent to Shenzhen. The exposure levels in all cities remained high because of the high mean $PM_{2.5}$ concentrations and their positive PPCE. To better protect public health, control efforts should target densely populated areas and city planning should locate more people in cleaner areas.

Keywords: $PM_{2.5}$; Public health; Satellite observation; Environmental policy; City planning

1. Introduction

Long-term exposure to outdoor particulate matter with an aerodynamic diameter of <2.5 μm ($PM_{2.5}$) is associated with a range of adverse health effects [1–5]. The level of population exposure to outdoor $PM_{2.5}$ in China is much higher than that in the U.S. or Europe [6]. As one of the major city clusters in China, the Pearl River Delta (PRD) region is exposed to a high level of $PM_{2.5}$ pollution [7]. The population-weighted mean $PM_{2.5}$ concentrations have been extensively used by researchers as an indicator of the population exposure level [8–15]. It is estimated by averaging the ambient $PM_{2.5}$ concentration associated with each individual within the study region. Burnett et al. [16] assessed the global population exposure to outdoor $PM_{2.5}$ in 2015 and concluded that the population-weighted mean $PM_{2.5}$ concentrations varied from the lowest levels in Canada/U.S. (7.9 $\mu g/m^3$) to the highest levels in China (57.5 $\mu g/m^3$) and India (74.0 $\mu g/m^3$). Using satellite-derived $PM_{2.5}$ data, Lin et al. [17] estimated the population-weighted mean $PM_{2.5}$ concentration to be 43.9 $\mu g/m^3$ in the PRD region from 2000 to 2014. In addition, their results showed that 84.0% of the population lived in areas with $PM_{2.5}$ concentrations that exceeded the World Health Organization (WHO) Interim Target 1 (IT-1) or the Chinese National Ambient Air Quality Standard (NAAQS), both of which are 35 $\mu g/m^3$. In February 2019, the "Outline Development Plan for Guangdong-Hong Kong-Macao Greater Bay Area" (the Greater Bay Area (GBA) Plan) was promulgated, which emphasized green development in this region. The regulation of pollutant emissions was tightened to further alleviate air pollution.

The variations in the mean $PM_{2.5}$ concentration level directly affect a population's exposure level in any given city. During the past decade, the governments of Guangdong Province and Hong Kong promulgated a series of control measures to reduce the $PM_{2.5}$ concentration [18]. Using satellite observations, Ma et al. [19] showed that the mean $PM_{2.5}$ concentration in the GBA region remained relatively constant from 2004 to 2007 and decreased from 2008 to 2013. Another study reported that all cities in the GBA region experienced an increasing mean $PM_{2.5}$ concentration during the 10th Five-Year Plan (FYP) period (2001–2005) and a decreasing mean $PM_{2.5}$ concentration during the 11th (2006–2010) and 12th (2011–2015) FYP periods [20].

A decrease in the mean $PM_{2.5}$ concentration is not necessarily associated with a decreasing population exposure level for the city if the $PM_{2.5}$ concentrations decrease in vast rural areas but increase in densely populated urban areas. The spatial differences in $PM_{2.5}$ changes therefore play an important role in exposure management [21]. Ideally, control efforts to reduce the $PM_{2.5}$ concentration should target densely populated urban areas. Lin et al. [22] assessed the differences in $PM_{2.5}$ variations between urban and rural areas for Chinese provinces, and they showed that the urban areas in the GBA region experienced a greater decrease in the $PM_{2.5}$ concentration than did rural areas during the 11th and 12th FYP periods. This type of spatial difference in $PM_{2.5}$ change assists a region to reduce its population exposure level.

Rapid urbanization typically leads to population migration into large urban areas. As reported by the Chinese statistical yearbook, the urban population in Guangdong Province increased from 47.5 million (55% of total population) in 2000 to 74.5 million (69% of total population) in 2015 (http://www.stats.gov.cn/tjsj/ndsj/). As urban areas are typically highly polluted, the migration of people to the urban areas in the GBA region during the past decade tended to increase its overall population exposure level. Ideally, demographic changes can reduce the exposure level if city planners relocate the population away from polluted areas. Further scientific and quantitative investigation of the impact of demographic change is needed.

The variations in the population exposure level are therefore determined by changes in the mean $PM_{2.5}$ concentration, spatial differences in $PM_{2.5}$ change and demographic changes. The level of population exposure to $PM_{2.5}$ for a city decreases if: (1) the mean $PM_{2.5}$ concentration declines, (2) urban areas experience a greater reduction of $PM_{2.5}$ concentration than rural areas, or (3) city planners relocate people away from polluted areas. To better guide public policies that aim to reduce exposure levels, it is essential to explicitly decompose and assess the impact of different factors.

Traditional studies have used ground-based networks to monitor the $PM_{2.5}$ concentration. However, such monitoring in China is much more limited than in developed countries [23]. Satellite remote sensing is an important step toward filling this data gap [24–26]. This study took advantage of high-resolution satellite observations to characterize long-term variations in human exposure to $PM_{2.5}$ for cities in the GBA region during the three most-recent FYP periods (2001–2015). A new decomposition method was then used to assess the impact of $PM_{2.5}$ variations and demographic changes on the exposure variation. Finally, suggestions for future environmental policies and urbanization planning were developed.

2. Data

2.1. Population Density

The GBA region of China contains nine major cities in Guangdong Province [Guangzhou (GZ), Shenzhen (SZ), Zhuhai (ZH), Dongguan (DG), Foshan (FS), Zhongshan (ZS), Zhaoqing (ZQ), Jiangmen (JM) and Huizhou (HZ)]. Guangzhou is the capital city of Guangdong Province. Shenzhen and Zhuhai are two special economic zones of China. The GBA region also contains two special administrative zones of China [i.e., Hong Kong (HK) and Macau (MC)]. All eleven administrative regions as cities were considered.

The yearly population density data was obtained at a spatial resolution of 1 km for the GBA region for 2001 and 2015 from the LandScan population database (http://web.ornl.gov/sci/landscan/). LandScan population data was constructed with the use of spatial data and imagery analyses to disaggregate census counts within administrative boundaries. A linear interpolation method was then applied to derive population densities for other years of the study period. The year- and city-specific gross population data were obtained from 2001 to 2015 from local statistical yearbooks (http://www.gdstats.gov.cn/). The LandScan-derived population data were adjusted by year- and city-specific factors to match the gross populations from the statistical yearbooks. Figure 1 shows the spatial distribution of the 15-year mean of population density in the GBA region. The population densities exceeded 10^3 persons/km^2 in urban areas of the GBA region.

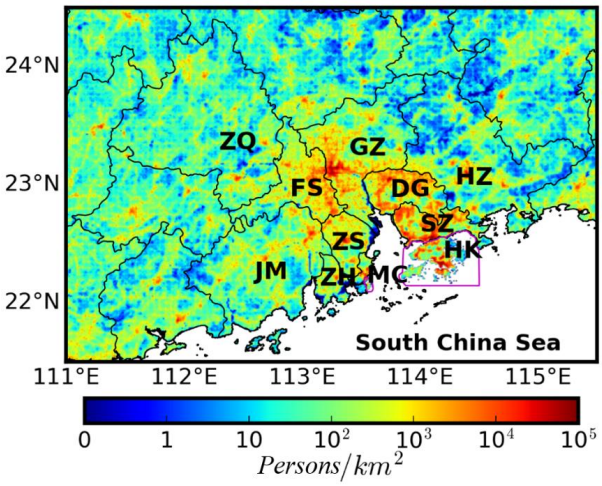

Figure 1. The spatial distribution of the 15-year mean of the population density at a spatial resolution of 0.01° × 0.01° in the Greater Bay Area (GBA) region of China.

2.2. Satellite-Derived $PM_{2.5}$

A high-resolution satellite-based $PM_{2.5}$ dataset was taken advantage of to characterize the long-term variations in the $PM_{2.5}$ concentration in the GBA region (http://envf.ust.hk/dataview/aod2pm/current). The algorithm was first used to build aerosol optical depth (AOD) data at a spatial resolution of 0.01° × 0.01° using spectral data from the two Moderate Resolution Imaging Spectroradiometer (MODIS) instruments aboard the Terra and Aqua satellites [27]. The verification

of the satellite-retrieved AOD against the ground-based sunphotometer observations showed retrieval errors within 15–20%. An observational data-driven AOD-$PM_{2.5}$ algorithm, which used ground-observed visibility and relative humidity data as inputs, was then applied to derive the ground-level $PM_{2.5}$ concentrations [28,29]. The uncertainty in the $PM_{2.5}$ concentrations resulted from the input data such as the AOD, meteorological values and model parameters. The evaluation of the satellite-derived $PM_{2.5}$ data against observations from the ground monitoring network within the GBA region during the entire study period identified the correlation coefficient, root mean square error, mean absolute bias and mean absolute percentage bias as 0.86 (N = 363), 4.7 μg/m^3, 3.6 ± 3.1 μg/m^3, and 9.3 ± 8.1%, respectively [20]. This accuracy is comparable to those with a correlation coefficient of 0.76–0.82 (N = 974–1145) in the U.S. and 0.74–0.79 (N = 45–68) in China for other existing long-term $PM_{2.5}$ data sets [11,30–32]. This study focused on residential areas with population densities of ≥10 persons/km^2. Figure 2 shows the spatial distribution of the 15-year mean of the $PM_{2.5}$ concentration in the residential areas of the GBA region. The $PM_{2.5}$ concentrations exceeded 60 μg/m^3 in the central GBA region.

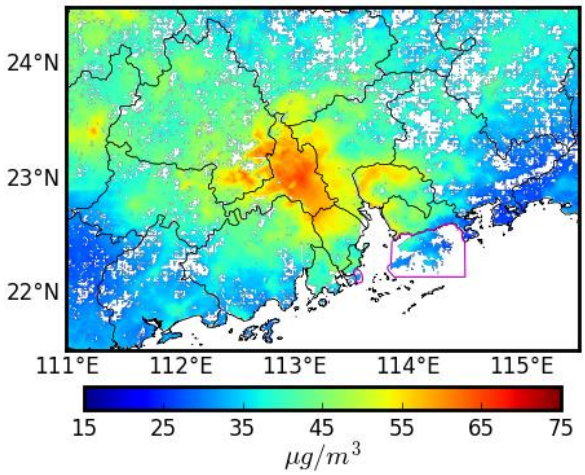

Figure 2. The spatial distribution of the 15-year mean of $PM_{2.5}$ concentration at a spatial resolution of 0.01° × 0.01° in the residential areas of the GBA region.

3. Methodology

The exposure decomposition framework is summarized as follows (more information can be found in the Appendix A). In a given region, the spatial distributions of $PM_{2.5}$ concentration and population density are denoted as $c_{i,j}$ and $\rho_{i,j}$, respectively, where $i = \{1, 2, 3, \ldots, X\}$ and $j = \{1, 2, 3, \ldots, Y\}$. The population-weighted mean $PM_{2.5}$ concentration (c_ρ) can be estimated by Equation (1):

$$c_\rho = \frac{\sum_{i=1}^{X}\sum_{j=1}^{Y} c_{i,j}\cdot\rho_{i,j}}{\sum_{i=1}^{X}\sum_{j=1}^{Y}\rho_{i,j}} \quad (1)$$

The spatial averages of the $PM_{2.5}$ concentration and population density in a region are represented by c_0 and ρ_0, respectively. The c_0 and ρ_0 values are estimated by averaging the $PM_{2.5}$ concentration and population density from all grids within the study region. Further, $c'_{i,j} = c_{i,j} - c_0$ and $p'_{i,j} = \frac{\rho_{i,j}-\rho_0}{\rho_0}$ was then defined as the deviation of the $PM_{2.5}$ concentration from c_0 and the relative deviation of population density from ρ_0, respectively. The $c'_{i,j}$ and $p'_{i,j}$ values therefore represent the differences in the $PM_{2.5}$ concentration and population density, respectively, from their regional average levels. The term c_ρ can be estimated by Equation (2):

$$c_\rho = c_0 + \frac{1}{A}\cdot\sum_{i=1}^{X}\sum_{j=1}^{Y} c'_{i,j}\cdot p'_{i,j} \quad (2)$$

where $A = X \cdot Y$ is the total grid number, representing the area of the study region. The authors defined $\boldsymbol{C'}$ and $\boldsymbol{P'}$ as the matrices of $c'_{i,j}$ and $p'_{i,j}$, respectively. The term $c_\rho$can then be expressed as Equation (3):

$$c_\rho = c_0 + \frac{1}{A} \cdot (\boldsymbol{C'} \cdot \boldsymbol{P'}) \tag{3}$$

An index of pollution-population-coincidence–induced $PM_{2.5}$ exposure (PPCE) of $c_1 = \frac{1}{A} \cdot (\boldsymbol{C'} \cdot \boldsymbol{P'})$ was introduced to represent the $PM_{2.5}$ exposure resulting from the spatial coincidence between the $PM_{2.5}$ concentration and population density. This PPCE is associated with the dot product of $\boldsymbol{C'}$ and $\boldsymbol{P'}$.

An increase in population density in polluted areas leads to a positive value of c_1, which increases the c_ρ level. Ideally, more people would reside in cleaner areas, which would be associated with a negative value of c_1. The trend in c_ρ can be expressed as Equation (4):

$$\frac{dc_\rho}{dt} = \frac{dc_0}{dt} + \frac{1}{A} \cdot \left(\boldsymbol{P'} \cdot \frac{d\boldsymbol{C'}}{dt} \right) + \frac{1}{A} \cdot \left(\boldsymbol{C'} \cdot \frac{d\boldsymbol{P'}}{dt} \right) \tag{4}$$

Equation (4) contains three parts: $\frac{dc_{\rho 1}}{dt} = \frac{dc_0}{dt}$; $\frac{dc_{\rho 2}}{dt} = \frac{1}{A} \cdot \left(\boldsymbol{P'} \cdot \frac{d\boldsymbol{C'}}{dt} \right)$; and $\frac{dc_{\rho 3}}{dt} = \frac{1}{A} \cdot \left(\boldsymbol{C'} \cdot \frac{d\boldsymbol{P'}}{dt} \right)$. The combination of the second and third parts represents the trend in PPCE (dc_1/dt). The c_ρ value decreases under three conditions: $\frac{dc_0}{dt} < 0$; $\boldsymbol{P'} \cdot \frac{d\boldsymbol{C'}}{dt} < 0$; or $\boldsymbol{C'} \cdot \frac{d\boldsymbol{P'}}{dt} < 0$. The first condition occurs if the mean $PM_{2.5}$ concentration decreased; the second condition occurs if densely populated urban areas experience a greater reduction of $PM_{2.5}$ concentration than rural areas; the third condition occurs if city planners relocate people from polluted areas to clean areas. These conditions are associated with the respective effects of the change in the mean $PM_{2.5}$ concentration, the spatial difference in $PM_{2.5}$ change and the demographic change.

4. Results

4.1. 15-Year Mean Population Exposure

Based on the 15-year averages of the $PM_{2.5}$ concentration and population density, Figure 3a,b show the deviation of the $PM_{2.5}$ concentration ($\boldsymbol{C'}$) and the relative deviation of population density ($\boldsymbol{P'}$), respectively, for different cities in the GBA region. The $c'_{i,j}$ or $p'_{i,j}$ values were positive (in red) in areas where the $PM_{2.5}$ concentration or population density was higher than the city's averages. It is noted that the population density in urban areas could be several times larger than the city average.

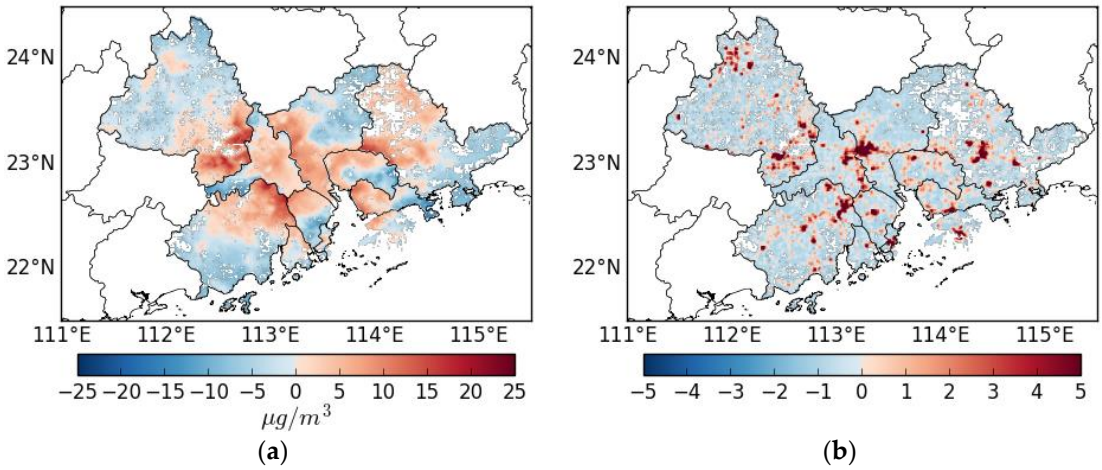

Figure 3. The 15-year averages of (**a**) the deviation of $PM_{2.5}$ concentration ($\boldsymbol{C'}$) and (**b**) the normalized deviation of population density ($\boldsymbol{P'}$) for different cities in the GBA region.

Figure 4 shows the 15-year average of PPCE for different cities in the GBA region. Ideally, the PPCE values should be negative. However, all cities had a positive PPCE value because of a positive spatial coincidence between the $PM_{2.5}$ concentration and population density. Hong Kong and Zhuhai had the lowest PPCE (c_1 = 1.3 μg/m^3). In contrast, the highest PPCE was found in Guangzhou (c_1 = 5.9 μg/m^3).

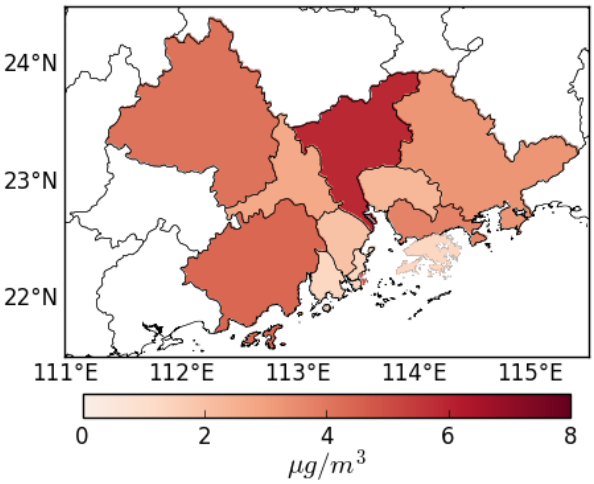

Figure 4. The 15-year average of pollution-population-coincidence–induced $PM_{2.5}$ exposure (PPCE) (c_1) for different cities in the GBA region.

The blue and red bars in Figure 5 show the 15-year averages of the mean $PM_{2.5}$ concentration (c_0) and the population-weighted mean $PM_{2.5}$ concentration (c_ρ), respectively, for different cities in the GBA region. The c_0 values were the lowest in Hong Kong (c_0 = 33.2 μg/m^3) and Macau (c_0 = 33.9 μg/m^3). In contrast, Foshan experienced the highest concentration of c_0 (57.1 μg/m^3). The high mean $PM_{2.5}$ concentrations and the positive PPCE values resulted in high levels of population exposure. The highest c_ρ values were found in the central GBA region: Foshan (c_ρ = 59.8 μg/m^3) and Guangzhou (c_ρ = 51.9 μg/m^3). These values were much higher than the WHO air-quality standards for annual $PM_{2.5}$ concentration, including those for IT-1 (35 μg/m^3), IT-2 (25 μg/m^3), IT-3 (15 μg/m^3) and Air Quality Guideline (AQG, 10 μg/m^3). Although the lowest c_ρ value (34.5 μg/m^3 in Hong Kong) did not exceed the WHO IT-1, it was still much higher than the WHO IT-2, IT-3 and AQG.

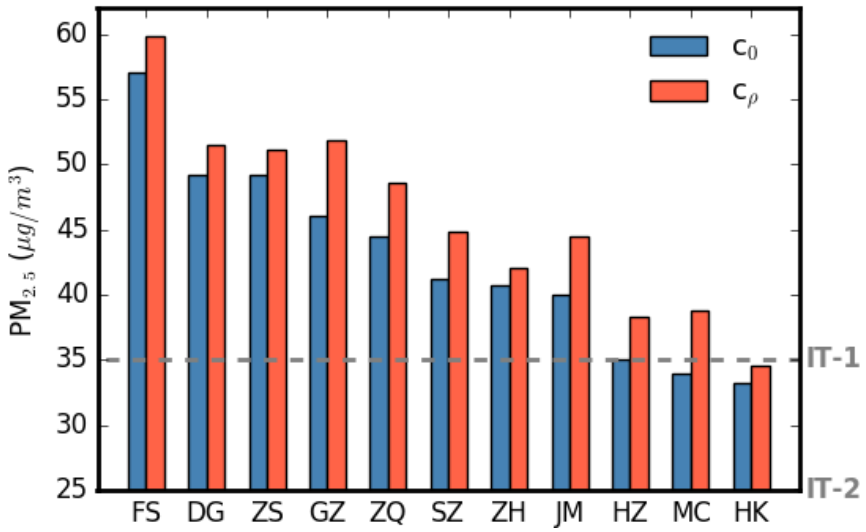

Figure 5. The 15-year averages of the mean $PM_{2.5}$ concentration (c_0, blue bars) and the population-weighted mean $PM_{2.5}$ concentration (c_ρ, red bars) for different cities in the GBA region. The cities are ordered according to their c_0 values.

4.2. Decomposition of Exposure Variation

4.2.1. Effect of Changes in Mean $PM_{2.5}$ Concentration

Figure 6 shows the trends in the population-weighted mean $PM_{2.5}$ concentration resulting from changes in the mean $PM_{2.5}$ concentration ($\frac{dc_{\rho_1}}{dt} = \frac{dc_0}{dt}$) for different cities in the GBA region during the three most-recent FYP periods. During the 10th FYP period, all cities experienced an increase in c_0. The most substantial increase in c_ρ resulting from increasing c_0 was observed in Foshan, where the concentration increased by 2.77 μg/m^3/year. During the 11th and 12th FYP periods, all cities experienced a decrease in c_0. The most substantial reduction of c_ρ resulting from decreasing c_0 was observed in Foshan, where the exposure level decreased by −2.25 μg/m^3/year during the 11th FYP period and in Zhongshan, where the exposure level decreased by −3.71 μg/m^3/year during the 12th FYP period.

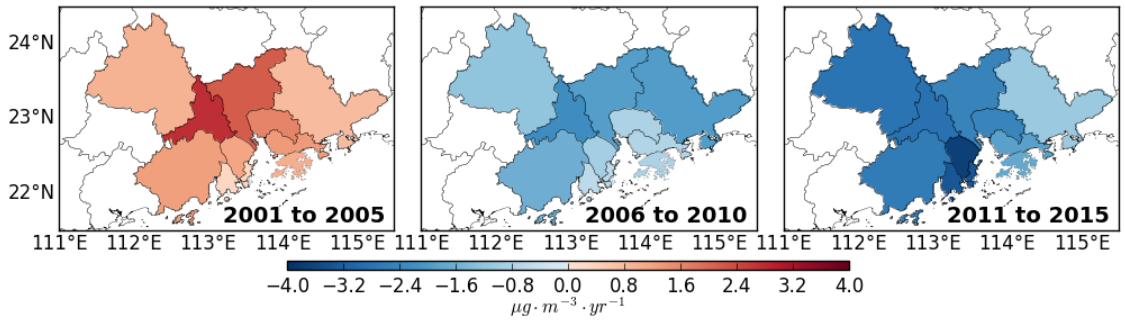

Figure 6. Trends in the population-weighted mean $PM_{2.5}$ concentration resulting from changes in the mean $PM_{2.5}$ concentration ($\frac{dc_{\rho_1}}{dt} = \frac{dc_0}{dt}$) for different cities in the GBA region during the three most-recent Five-Year Plan (FYP) periods.

4.2.2. The Effect of Spatial Differences in $PM_{2.5}$ Change

Figure 7a shows the trends in the deviation of the $PM_{2.5}$ concentration ($d\boldsymbol{C}'/dt$) for different cities during the three most-recent FYP periods. The areas with increasing $c'_{i,j}$ values (in red) experienced less of a reduction of the $PM_{2.5}$ concentration than those with decreasing $c'_{i,j}$ values (in blue). During the 10th FYP period, densely populated urban areas ($p'_{i,j} > 0$) experienced greater increases in the $PM_{2.5}$ concentration than rural areas ($p'_{i,j} < 0$) in most cities (8 out of 11). As a result, the spatial difference in the $PM_{2.5}$ change increased c_ρ in these cities. The left panel of Figure 7b shows the trends in the population-weighted mean $PM_{2.5}$ concentration resulting from the spatial difference in the $PM_{2.5}$ change [$\frac{dc_{\rho_2}}{dt} = \frac{1}{A} \cdot \left(\boldsymbol{P}' \cdot \frac{d\boldsymbol{C}'}{dt}\right)$] for different cities during the 10th FYP period. The most substantial increase in c_ρ resulting from the spatial difference in the $PM_{2.5}$ change was observed in Guangzhou, where the exposure level increased by 1.03 μg/m^3/year.

During the 11th and 12th FYP periods, densely populated urban areas ($p'_{i,j} > 0$) experienced a greater decline in the $PM_{2.5}$ concentration than rural areas ($p'_{i,j} < 0$) in most cities (7 and 10 cities, respectively). As a result, the spatial difference in the $PM_{2.5}$ change reduced c_ρ in these cities. The middle and right panels of Figure 7b show the trends in the population-weighted mean $PM_{2.5}$ concentration resulting from the spatial difference in $PM_{2.5}$ change for different cities during the 11th and 12th FYP periods, respectively. During the 11th FYP period, the effect reduced c_ρ most substantially in Guangzhou, where the exposure level decreased by −0.31 μg/m^3/year. During the 12th FYP period, the effect reduced c_ρ most substantially in Macau, where the exposure level decreased by −0.58 μg/m^3/year and in Shenzhen, where the exposure level decreased by −0.42 μg/m^3/year.

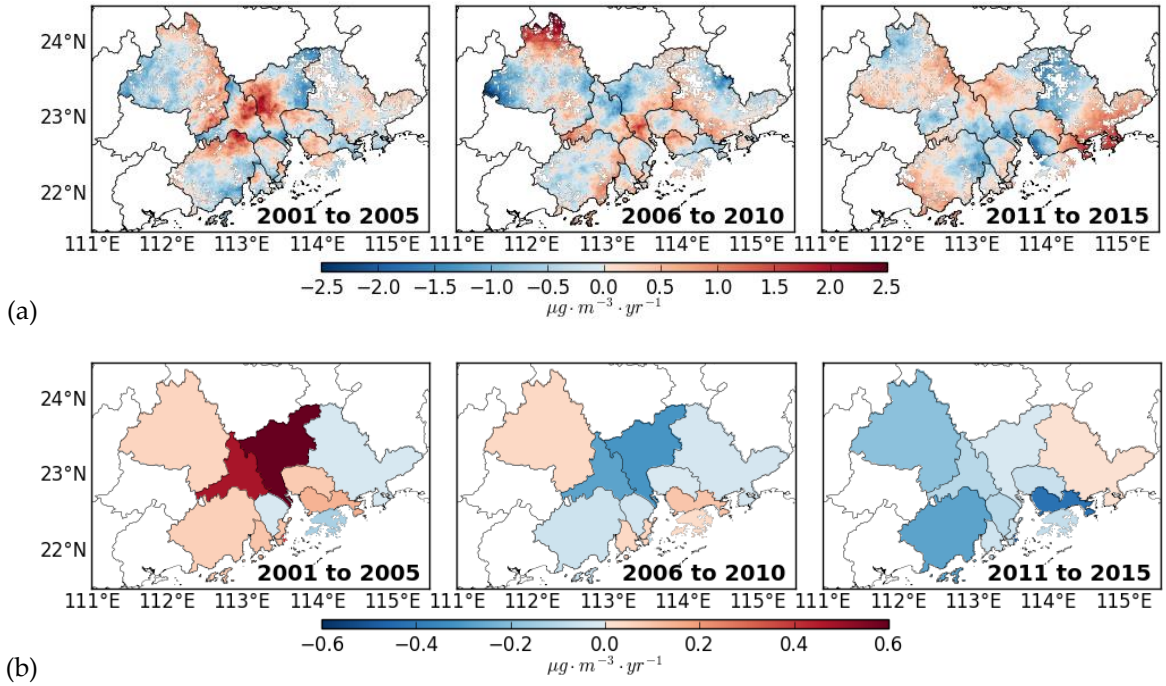

Figure 7. (**a**) Trends in the deviation of the $PM_{2.5}$ concentration ($d\boldsymbol{C}'/dt$) for different cities during the three most-recent FYP periods. (**b**) Trends in the population-weighted mean $PM_{2.5}$ concentration resulting from the spatial differences in $PM_{2.5}$ changes [$\frac{dc_{\rho_2}}{dt} = \frac{1}{A} \cdot \left(\boldsymbol{P}' \cdot \frac{d\boldsymbol{C}'}{dt}\right)$] for different cities during the three most-recent FYP periods.

4.2.3. The Effect of Demographic Change

Figure 8a plots trends in the relative deviation of population density ($d\boldsymbol{P}'/dt$) for different cities in the GBA region during the three most-recent FYP periods. The areas with increasing $p'_{i,j}$ values (in red) experienced a greater percentage increase in the population density than those with decreasing $p'_{i,j}$ values (in blue). It was found that urban areas in most cities experienced an increase in $p'_{i,j}$ value. As these urban areas were typically more polluted than the rural areas, the increasing $p'_{i,j}$ value in urban areas (typically with $c'_{i,j} > 0$) increased c_ρ in these cities. Figure 8b plots trends in the population-weighted mean $PM_{2.5}$ concentration resulting from the demographic changes [$\frac{dc_{\rho_3}}{dt} = \frac{1}{A} \cdot \left(\boldsymbol{C}' \cdot \frac{d\boldsymbol{P}'}{dt}\right)$] for different cities in the GBA region during the three most-recent FYP periods. The effect increased c_ρ by as much as 0.18 μg/m^3/year.

Dongguan was a special case, in which the demographic change decreased c_ρ [i.e., $\frac{1}{A} \cdot \left(\boldsymbol{C}' \cdot \frac{d\boldsymbol{P}'}{dt}\right) < 0$] by as much as −0.10 μg/m^3/year during the three FYP periods studied. Figure 9a shows the 15-year trend in the relative deviation of the population density ($d\boldsymbol{P}'/dt$) from 2001 to 2015 in Dongguan. It was found that the southeastern region experienced a greater increase of the population density than the northwestern region. To evaluate this demographic change, gross population data was collected for different towns in Dongguan from the statistical yearbook (http://tjj.dg.gov.cn). The ratios of the gross population for 2001 and 2015 in different towns are shown in Figure 10. The results showed that towns southeast of the city adjacent to Shenzhen experienced a greater percentage increase in population than those in the northwest. This population change characteristic is consistent with that using the gridded data.

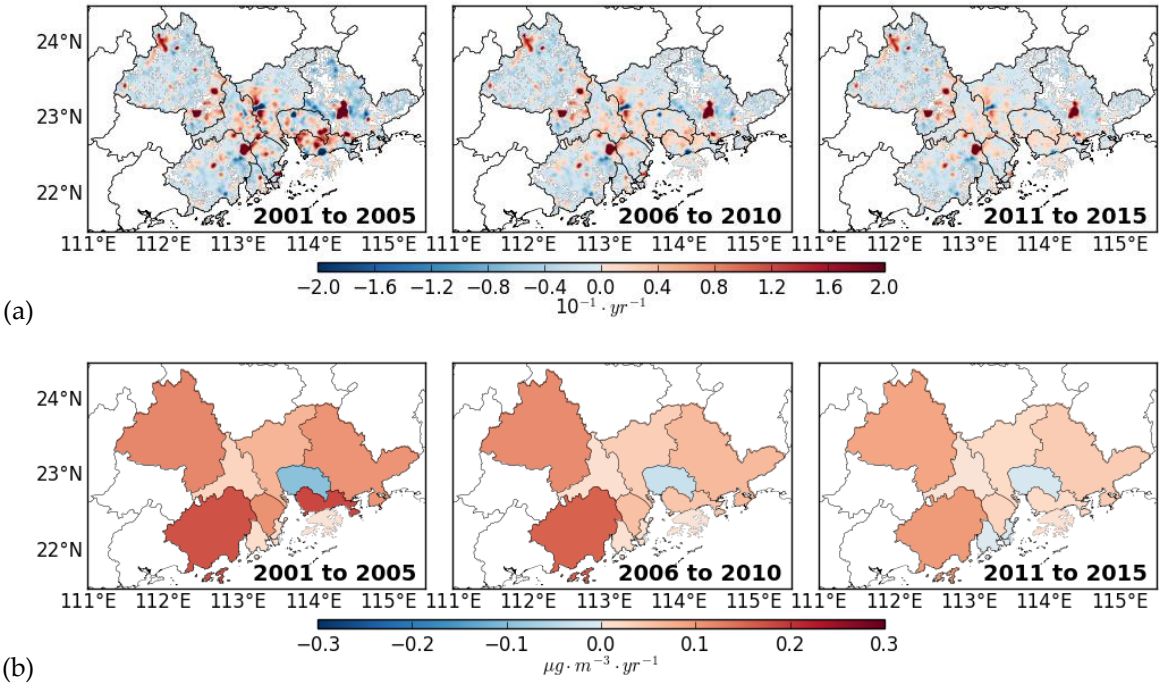

Figure 8. (**a**) Trends in the relative deviation of the population density ($d\boldsymbol{P}'/dt$) for different cities in the GBA region during the three most-recent FYP periods. (**b**) Trends in the population-weighted mean $PM_{2.5}$ concentration resulting from demographic changes [$\frac{dc_{p_3}}{dt} = \frac{1}{A} \cdot \left(\boldsymbol{C}' \cdot \frac{d\boldsymbol{P}'}{dt}\right)$] for different cities in the GBA region during the three most-recent FYP periods.

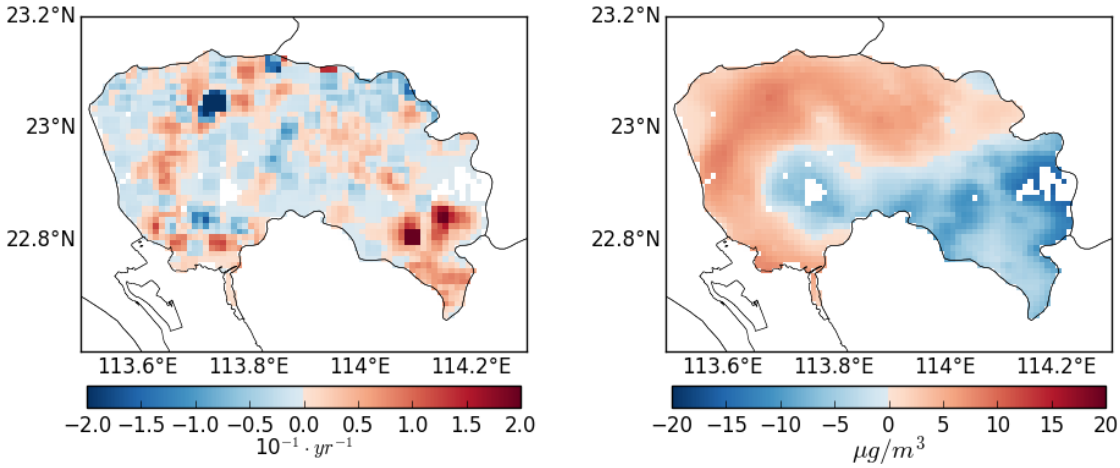

Figure 9. (**a**) The trend in the relative deviation of the population density ($d\boldsymbol{P}'/dt$) from 2001 to 2015 in Dongguan. (**b**) The 15-year average of the deviation of the $PM_{2.5}$ concentration ($\boldsymbol{C}'$) in Dongguan.

Based on the 15-year average of $PM_{2.5}$ concentration, Figure 9b shows the deviation of the $PM_{2.5}$ concentration ($\boldsymbol{C}'$) in Dongguan. Higher $PM_{2.5}$ concentrations were observed in the northwestern region, whereas lower $PM_{2.5}$ concentrations were observed in the southeastern region. These results indicate that Dongguan rapidly developed residential areas in the cleaner regions that were adjacent to Shenzhen during the past decade. This demographic change pattern helped Dongguan reduce its population $PM_{2.5}$ exposure level.

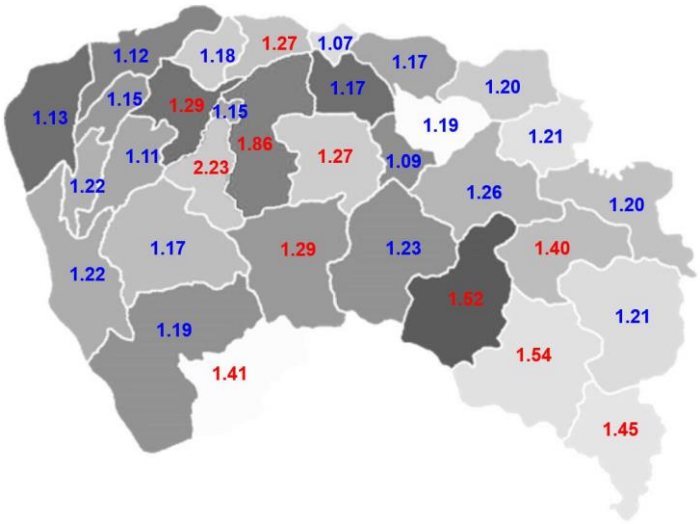

Figure 10. The ratios of gross population for 2001 and 2015 for different towns in Dongguan. The numbers in red indicate towns with ratios that were higher than the city average. In contrast, the numbers in blue indicate towns with ratios that were lower than the city average.

4.2.4. Long-Term Variation in PPCE

The variation in PPCE was determined by the combined effect of spatial differences in $PM_{2.5}$ changes and demographic changes. Figure 11 shows the inter-annual variations in PPCE for different cities in the GBA region from 2001 to 2015. Most cities experienced an increase in PPCE during the 10th FYP period and a decrease in PPCE during the 12th FYP period. It is encouraging to find that the PPCE levels decreased to approximately half the previous maximum in most cities except in a few non-central cities such as Zhaoqing, Jiangmen and Huizhou. In 2015, the PPCE levels were still positive in all cities. The maximum PPCE levels in 2015 were found in Zhaoqing (3.7 μg/m^3), Guangzhou (3.4 μg/m^3) and Huizhou (3.2 μg/m^3).

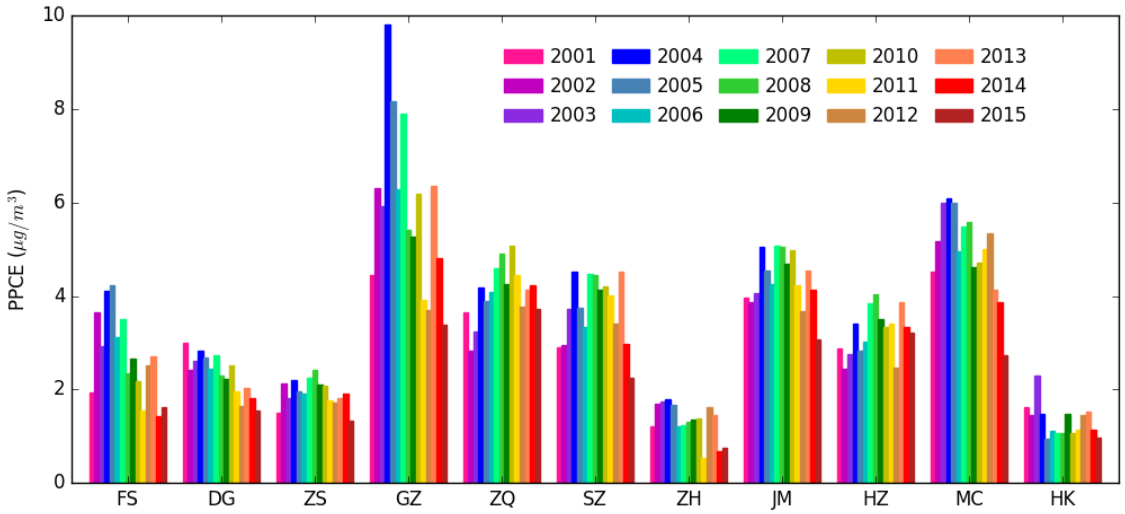

Figure 11. Inter-annual variations in the PPCE for different cities in the GBA region from 2001 to 2015.

4.2.5. The Long-Term Variations in Population Exposure

The variations in the population-weighted mean $PM_{2.5}$ concentration (c_ρ) were determined by the combined effect of changes in the mean $PM_{2.5}$ concentration, spatial differences in $PM_{2.5}$ change and demographic changes. Figure 12 shows inter-annual variations in c_ρ for different cities in the GBA region from 2001 to 2015. In general, the c_ρ values started to decrease during the 11th and 12th FYP

periods in all cities. However, in 2015, the c_ρ values remained high in all cities. Although the lowest c_ρ value (c_ρ = 25.9 μg/m^3 in Hong Kong) was lower than that of WHO IT-1, it still exceeded those of WHO IT-2, IT-3 and AQG.

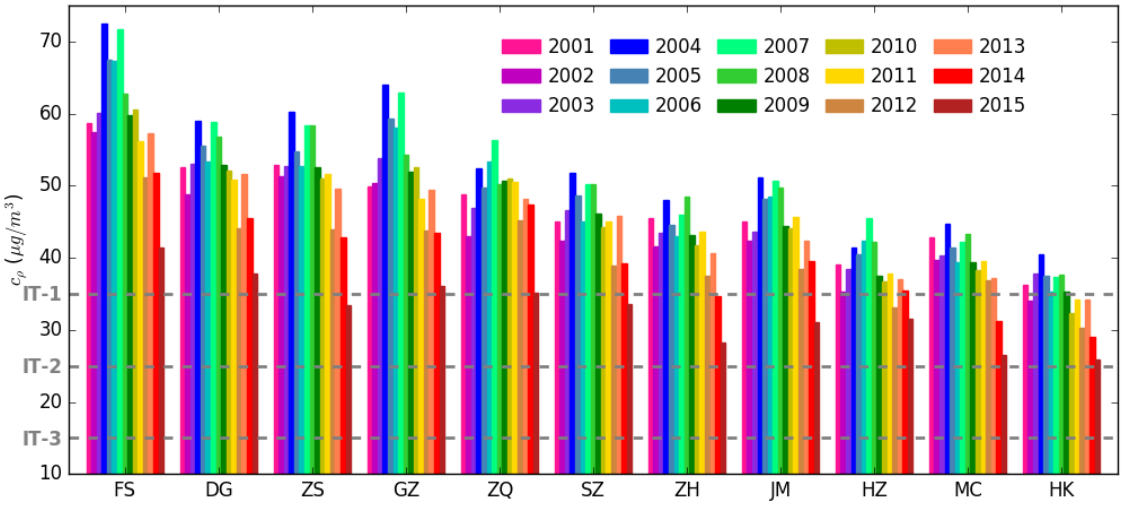

Figure 12. The inter-annual variations in the population-weighted mean $PM_{2.5}$ concentration (c_ρ) for different cities in the GBA region from 2001 to 2015.

Figure 13 shows the trends in the population-weighted mean $PM_{2.5}$ concentration (dc_ρ/dt) resulting from the combined effect for different cities in the GBA region during the three most-recent FYP periods. During the 10th FYP period, c_ρ increased in all cities. The most substantial increases in c_ρ were observed in Foshan, where the exposure level increased by 3.27 μg/m^3/year and in Guangzhou, where the exposure level increased by 3.28 μg/m^3/year. During the 11th and 12th FYP periods, c_ρ declined in all cities. The reduction in c_ρ was the most substantial in Foshan, where the exposure level decreased by −2.53 μg/m^3/year during the 11th FYP period, and in Zhongshan, where the exposure level decreased by −3.78 μg/m^3/year during the 12th FYP period.

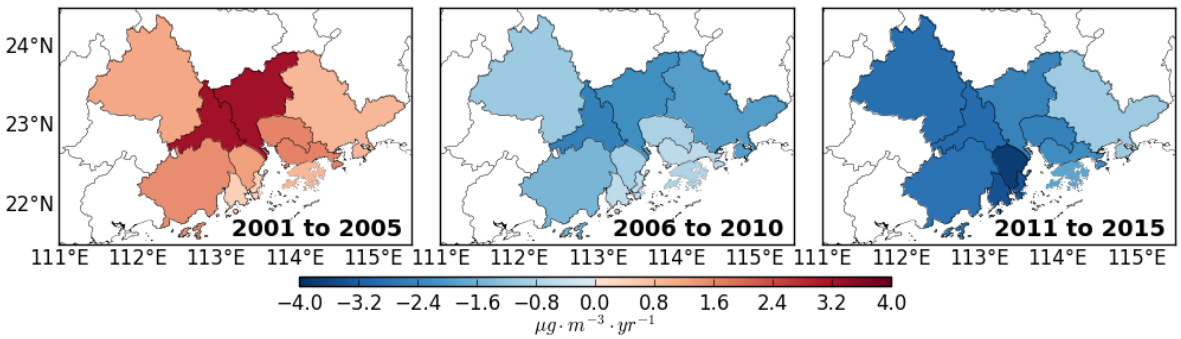

Figure 13. The trends in the population-weighted mean $PM_{2.5}$ concentration (dc_ρ/dt) for different cities in the GBA region during the three FYP periods.

5. Discussion

Lin et al. [17] compared the spatial mean and population-weighted mean $PM_{2.5}$ concentrations for the cities in the GBA region from 2000 to 2014 and found that the population-weighted mean $PM_{2.5}$ concentrations were systematically higher than the spatial averages. The systematic differences were related to the positive spatial correlation between the $PM_{2.5}$ concentration and population density. For the entire GBA region, the population-weighted mean $PM_{2.5}$ concentration was higher than the spatial average by 5.9 μg/m^3. This study further investigated the characteristics of this difference using the pollution-population-coincidence induced $PM_{2.5}$ exposure (PPCE). The PPCE is an important part

of the population exposure level not only because its current level is significantly high, but also because its optimal level should be negative.

The mean $PM_{2.5}$ concentration levels in all cities of the GBA region of China decreased during the 11th and 12th FYP periods, due to the implementation of improved control measures. In addition to the beneficial effect of the decreasing mean $PM_{2.5}$ concentrations, it was found that spatial differences in the $PM_{2.5}$ changes also reduced the population exposure levels in most cities during the 11th and 12th FYP periods. In contrast, demographic changes increased the exposure levels in most cities because of their rapid urbanization. Dongguan was a special case that experienced the best city planning in terms of reducing population exposure. The rapid development of residential areas in cleaner regions adjacent to Shenzhen reduced its population exposure level during the past decade.

Although the population exposure levels greatly decreased for cities in the GBA region during the past decade, their levels remained high because of the high mean $PM_{2.5}$ concentrations and a positive PPCE. To better protect public health, more control efforts are required to reduce both the mean $PM_{2.5}$ concentration and PPCE. Currently, the reduction of the mean $PM_{2.5}$ concentration contributes significantly to the reduction of exposure levels in the GBA region. However, further reduction in the mean $PM_{2.5}$ concentration becomes more difficult as it drops to a lower level. The positive PPCE levels in all cities suggest that unfavorable city planning has located residential dwellings in polluted areas. To reduce PPCE, it is suggested that control efforts further target densely populated areas (e.g., controls of mobile and residential sources) and that city planners relocate some sources of pollution (e.g., emissions from industrial sources or power generation) away from these densely populated urban areas and locate more residential dwellings in cleaner areas.

It is difficult to find a truly objective criterion to classify a geographical area as urban or rural. All classification methods require a choice of threshold, which is subjective to a certain extent. The Organization for Economic Co-operation and Development (OECD) uses population size cutoffs (50,000 or 100,000 people) and population density cutoffs (1000 or 1500 persons/km^2 depending on the country) to define urban cores [33]. Following the OECD approach, Lin et al. [22] used the population density threshold of 1500 persons/km^2 for the classification of urban and rural areas, and investigated the differences in $PM_{2.5}$ variations between urban and rural areas for provinces in China. Their results showed that the urban areas in the GBA region experienced a greater increase in the $PM_{2.5}$ concentration than did rural areas during the 10th FYP period and a greater decrease in $PM_{2.5}$ concentration than did rural areas during the 11th and 12th FYP periods. These results are consistent with this study showing that the spatial difference in the $PM_{2.5}$ change increased population exposure levels in most cities during the 10th FYP period and reduced population exposure levels in most cities during the 11th and 12th FYP periods.

The uncertainties of exposure assessment might result from both the $PM_{2.5}$ concentration and population density. The evaluation of the satellite-derived $PM_{2.5}$ concentration against ground observations in the GBA region obtained a correlation coefficient of 0.86 and a mean percentage bias of <20% [20]. To reduce the bias of the LandScan-derived population density data, the gridded population data was adjusted using gross population data collected from the statistical yearbooks. The assessment in this study focused on residential areas with population densities of ≥10 persons/km^2. These residential areas contained 99.9% of the total population within the study region.

This study was focused on the decomposition of long-term variations in the population exposure to outdoor $PM_{2.5}$, which were measured using a satellite remote sensing technique. The exposure to indoor $PM_{2.5}$ would also negatively impact human health [34]. The indoor and outdoor exposure levels differ because of factors such as the spatial variability of the $PM_{2.5}$ concentration and outdoor-to-indoor infiltration. The measurement of indoor pollution exposure requires advanced and portable sensor devices [35,36]. Future studies could assess the indoor exposure and its health impact using the sensor measurements.

The climate in the GBA region is affected by seasonal monsoons. The prevailing winds are from the north in winter and from the south in summer. The monsoons affect the monthly variation in

the $PM_{2.5}$ concentration in this region. Based on the satellite-derived monthly $PM_{2.5}$ data, Figure 14 shows the monthly variation of the population-weighted mean $PM_{2.5}$ concentration for different cities during the study period. All cities experienced lower population exposure levels in summer and higher population exposure levels in winter. The highest population exposure levels were typically found in January and December, with a level as high as >60 μg/m^3 for cities in central GBA region (e.g., Foshan and Guangzhou). The population exposure levels actually doubled from summer to winter in several cities such as Zhongshan, Zhuhai and Jiangmen. Stronger regional transport of pollutants from inland, fewer mixing layers and less precipitation leads to higher levels of $PM_{2.5}$ exposure in winter than in summer [17].

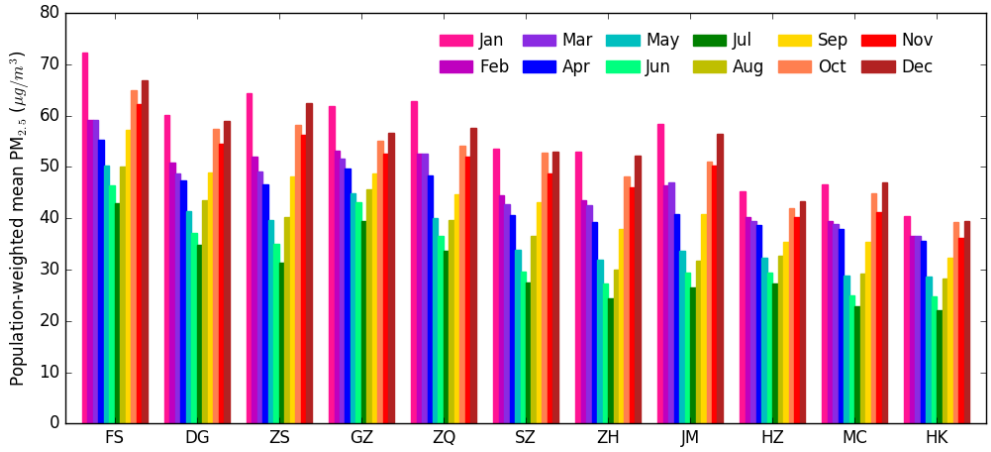

Figure 14. The monthly variation in the population-weighted mean $PM_{2.5}$ concentration (c_ρ) for different cities in the GBA region during the entire study period.

The highly developed economy and industry in the GBA region offer a large number of employment opportunities. Therefore, many residents in the GBA region come from other provinces and work in this region. During the Chinese New Year, which is usually a one-week holiday in February, most of these people move back to their hometowns. The movement of these people changes their short-term exposure levels. The changes are determined by the differences in the $PM_{2.5}$ concentration level between the GBA region and their hometowns. Future studies could collect detailed information on the movement of populations over specific short-term periods and assess its effect on population exposure level.

The rapid economic development and urbanization in the GBA region has also caused complex environmental and health challenges from other air pollutants, such as sulfur dioxide (SO_2), nitrate oxides (NO_x) and ozone [37–39]. To better guide local environmental policies, it would be of great value to assess the population exposure to other air pollutants and the factors that influence such exposure. Further research could delineate exposure decompositions for other air pollutants in the study region.

6. Conclusions

This study used a decomposition method to assess the impact of $PM_{2.5}$ variations and demographic changes on the exposure variations for cities in the GBA region of China during the three most-recent FYP periods. This study took advantage of high-resolution satellite observations to characterize the long-term variation in human exposure to $PM_{2.5}$. The results showed that the 15-year average PPCE levels were positive in all cities, suggesting that unfavorable city planning had placed people in the polluted areas. The analyses of the spatial differences in $PM_{2.5}$ changes showed that urban areas experienced a greater decrease in the $PM_{2.5}$ concentration than rural areas did in most cities during the 11th (2006–2010) and 12th (2011–2015) FYP periods. These spatial differences in $PM_{2.5}$ changes reduced their PPCE levels and thus reduced the exposure levels. The migration of population resulting from rapid urbanization, however, increased the PPCE and exposure levels in most cities during

the three FYP periods considered. Dongguan was the only city in which the demographic change reduced the exposure level because of its rapid development of residential areas in cleaner regions adjacent to Shenzhen. The exposure levels in all cities remained high because of the high mean $PM_{2.5}$ concentrations and their positive PPCE. To better protect public health, control efforts should target densely populated areas and city planning should place more residential dwellings in cleaner areas.

Author Contributions: The composition of the manuscript was supervised by A.K.H.L.; C.L. (Changqing Lin) drafted the original manuscript; J.C.H.F., Q.H., J.M., X.L., Z.L., C.L. (Chengcai Li), R.Z. and A.H.S.W. edited the manuscript.

Funding: This work was supported by the Research Grants Council of Hong Kong Government (Project No. T24/504/17), the Science and Technology Plan Project of Guangdong Province of China (Grant No. 2017A050506003), NSFC/RGC (Grant N_HKUST631/05), and the Fok Ying Tung Graduate School (NRC06/07.SC01).

Acknowledgments: We thank the Hong Kong Environmental Protection Department for provision of air-quality monitoring data.

Conflicts of Interest: The authors declare no conflicts of interest. The funders had no role in the design of the study; in the collection, analyses, or interpretation of data; in the writing of the manuscript; or in the decision to publish the results.

Abbreviations

GBA	Greater Bay Area
PRD	Pearl River Delta
FYP	Five-Year Plan
AOD	Aerosol optical depth
$PM_{2.5}$	Fine particulate matter
MODIS	Moderate Resolution Imaging Spectroradiometer
WHO	World Health Organization
IT-1	Interim Target 1
IT-2	Interim Target 2
IT-3	Interim Target 3
AQG	Air Quality Guideline
NAAQS	Chinese National Ambient Air Quality Standard
GZ	Guangzhou city
SZ	Shenzhen city
ZH	Zhuhai city
DG	Dongguan city
FS	Foshan city
ZS	Zhongshan city
ZQ	Zhaoqing city
JM	Jiangmen city
HZ	Huizhou city
HK	Hong Kong special administrative zone
MC	Macau special administrative zone
c_ρ	Population-weighted mean $PM_{2.5}$ concentration
$c_{i,j}$	Spatial distribution of $PM_{2.5}$ concentration
$\rho_{i,j}$	Spatial distribution of population density
c_0	Spatial average of $PM_{2.5}$ concentration
ρ_0	Spatial average of population density
A	Area of the study region
$c'_{i,j}$	Deviation of $PM_{2.5}$ concentration from c_0
$\rho'_{i,j}$	Deviation of population density from ρ_0
$p'_{i,j}$	Relative deviation of population density from ρ_0
$\boldsymbol{C'}$	Matrix of $c'_{i,j}$
$\boldsymbol{P'}$	Matrix of $p'_{i,j}$
PPCE (c_1)	Pollution-population-coincidence–induced $PM_{2.5}$ exposure

Appendix A. Appendix: Exposure decomposition

In a two-dimensional region, the spatial distribution of $PM_{2.5}$ concentration is denoted as $c_{i,j}$ and population density is denoted as $\rho_{i,j}$, where $i = \{1, 2, 3, \ldots, X\}$ and $j = \{1, 2, 3, \ldots, Y\}$. This study used c_0 and ρ_0 to represent the spatial averages of the $PM_{2.5}$ concentration and population density, respectively, in the study region. They can be respectively expressed as Equations (A1.1) and (A1.2):

$$c_0 = \frac{1}{A}\sum_{i=1}^{X}\sum_{j=1}^{Y} c_{i,j} \tag{A1.1}$$

$$\rho_0 = \frac{1}{A}\sum_{i=1}^{X}\sum_{j=1}^{Y} \rho_{i,j} \tag{A1.2}$$

where $A = X{\cdot}Y$ is the total grid number, representing the area of the study region. Then, $c'_{i,j}$ and $\rho'_{i,j}$ are defined as the deviation of the $PM_{2.5}$ concentration from c_0 and the deviation of population density from ρ_0, respectively. They can be respectively expressed as Equations (A2.1) and (A2.2)

$$c'_{i,j} = c_{i,j} - c_0 \tag{A2.1}$$

$$\rho'_{i,j} = \rho_{i,j} - \rho_0 \tag{A2.2}$$

The $c'_{i,j}$ values are positive in polluted areas and negative in clean areas. The $\rho'_{i,j}$ values are positive in densely populated urban areas and negative in rural areas. By definition, Equations (A3.1) and (A3.2) are as follows:

$$\sum_{i=1}^{X}\sum_{j=1}^{Y} c'_{i,j} = 0 \tag{A3.1}$$

$$\sum_{i=1}^{X}\sum_{j=1}^{Y} \rho'_{i,j} = 0 \tag{A3.2}$$

The population-weighted mean $PM_{2.5}$ concentration (c_ρ) can be quantified by Equation (A4):

$$c_\rho = \frac{\sum_{i=1}^{X}\sum_{j=1}^{Y} c_{i,j}{\cdot}\rho_{i,j}}{\sum_{i=1}^{X}\sum_{j=1}^{Y} \rho_{i,j}} \tag{A4}$$

Or, it can be expressed as Equations (A5.1) and (A5.2):

$$c_\rho = \frac{\sum_{i=1}^{X}\sum_{j=1}^{Y} (c_0 + c'_{i,j}){\cdot}\left(\rho_0 + \rho'_{i,j}\right)}{\rho_0{\cdot}A} \tag{A5.1}$$

$$c_\rho = \frac{\sum_{i=1}^{X}\sum_{j=1}^{Y} (c_0{\cdot}\rho_0 + c_0{\cdot}\rho'_{i,j} + c'_{i,j}{\cdot}\rho_0 + c'_{i,j}{\cdot}\rho'_{i,j})}{\rho_0{\cdot}A} \tag{A5.2}$$

By separating out c_0, c_ρ can be expressed as Equations (A6.1) and (A6.2):

$$c_\rho = c_0 + \frac{\sum_{i=1}^{X}\sum_{j=1}^{Y} c'_{i,j}{\cdot}\rho'_{i,j}}{\rho_0{\cdot}A} \tag{A6.1}$$

$$c_\rho = c_0 + \frac{1}{A}{\cdot}\sum_{i=1}^{X}\sum_{j=1}^{Y} (c_{i,j} - c_0){\cdot}\frac{(\rho_{i,j} - \rho_0)}{\rho_0} \tag{A6.2}$$

Equation(A7) can be defined as:

$$p'_{i,j} = \frac{\rho_{i,j} - \rho_0}{\rho_0} \tag{A7}$$

to represent the normalized deviation of the population density from ρ_0. c_ρ can then be expressed as Equation (A8):

$$c_\rho = c_0 + \frac{1}{A} \cdot \sum_{i=1}^{X} \sum_{j=1}^{Y} {c'}_{i,j} \cdot {p'}_{i,j} \tag{A8}$$

Furthermore, $\boldsymbol{C'}$ and $\boldsymbol{P'}$ are defined as Matrices of ${c'}_{i,j}$ and ${p'}_{i,j}$, respectively. Then, c_ρ can be expressed as Equation (A9):

$$c_\rho = c_0 + \frac{1}{A} \cdot (\boldsymbol{C'} \cdot \boldsymbol{P'}) \tag{A9}$$

The c_ρ value is therefore determined by the mean $PM_{2.5}$ concentration (c_0) together with a dot product of the deviation of the $PM_{2.5}$ concentration ($\boldsymbol{C'}$) and the normalized deviation of the population density ($\boldsymbol{P'}$). The second part of c_ρ is associated with the spatial coincidence between the population density and $PM_{2.5}$ concentration. A pollution-population-coincidence–induced $PM_{2.5}$ exposure (PPCE) of c_1 was used to represent the $PM_{2.5}$ exposure resulting from this effect. This PPCE (c_1) can be expressed as Equation (A10):

$$c_1 = \frac{1}{A} \cdot (\boldsymbol{C'} \cdot \boldsymbol{P'}) \tag{A10}$$

c_ρ can then be expressed as Equation (A11):

$$c_\rho = c_0 + c_1 \tag{A11}$$

The c_ρ value can be decomposed into two parts. The first part is the mean $PM_{2.5}$ concentration (c_0) and the second part is PPCE (c_1). An increase in population density in polluted areas leads to a positive value of c_1, which boosts the c_ρ level. To lessen the human exposure to $PM_{2.5}$, the most successful control strategies must simultaneously decrease the mean $PM_{2.5}$ concentration (c_0) and the PPCE (c_1). The trend in c_ρ can be expressed as Equation (A12):

$$\frac{dc_\rho}{dt} = \frac{dc_0}{dt} + \frac{dc_1}{dt} \tag{A12}$$

The trend in c_1 can be expressed as Equation (A13):

$$\frac{dc_1}{dt} = \frac{1}{A} \cdot \left(\boldsymbol{P'} \cdot \frac{d\boldsymbol{C'}}{dt} \right) + \frac{1}{A} \cdot \left(\boldsymbol{C'} \cdot \frac{d\boldsymbol{P'}}{dt} \right) \tag{A13}$$

The elements of the trends in $\boldsymbol{C'}$ and $\boldsymbol{P'}$ can be expressed as Equations (A14.1) and (A14.2):

$$\frac{d{c'}_{i,j}}{dt} = \frac{d\left(c_{i,j} - c_0\right)}{dt} = \frac{dc_{i,j}}{dt} - \frac{dc_0}{dt} \tag{A14.1}$$

$$\frac{d{p'}_{i,j}}{dt} = \frac{d\left(\frac{\rho_{i,j} - \rho_0}{\rho_0}\right)}{dt} = \frac{\rho_{i,j}}{\rho_0} \left(\frac{1}{\rho_{i,j}} \frac{d\rho_{i,j}}{dt} - \frac{1}{\rho_0} \frac{d\rho_0}{dt} \right) \tag{A14.2}$$

The ${c'}_{i,j}$ values decline in areas where the $PM_{2.5}$ concentrations undergo a greater reduction than the average level. The ${p'}_{i,j}$ values decline in areas where the population densities undergo a greater percentage reduction than the average level. When ρ_0 is relatively stable (i.e., $\frac{d\rho_0}{dt} \approx 0$), the ${p'}_{i,j}$ values decrease in areas where population densities decrease (i.e., people migrate out of the area). In contrast, the ${p'}_{i,j}$ values increase in areas where population densities increase (i.e., people migrate into the areas).

The trend in c_ρ can then be expressed as Equation (A15):

$$\frac{dc_\rho}{dt} = \frac{dc_0}{dt} + \frac{1}{A} \cdot \left(\boldsymbol{P'} \cdot \frac{d\boldsymbol{C'}}{dt} \right) + \frac{1}{A} \cdot \left(\boldsymbol{C'} \cdot \frac{d\boldsymbol{P'}}{dt} \right) \tag{A15}$$

The trend in c_ρ can be decomposed into three parts (Equations (A16.1–16.3)):

$$\frac{dc_{\rho_1}}{dt} = \frac{dc_0}{dt} \tag{A16.1}$$

$$\frac{dc_{\rho_2}}{dt} = \frac{1}{A} \cdot \left(\boldsymbol{P'} \cdot \frac{d\boldsymbol{C'}}{dt} \right) \tag{A16.2}$$

$$\frac{dc_{\rho_3}}{dt} = \frac{1}{A}\cdot\left(\boldsymbol{C'}\cdot\frac{d\boldsymbol{P'}}{dt}\right) \quad \text{(A16.3)}$$

The c_ρ value therefore decreases under three conditions: (a) $\frac{dc_0}{dt} < 0$; (b) $\boldsymbol{P'}\cdot\frac{d\boldsymbol{C'}}{dt} < 0$; or (c) $\boldsymbol{C'}\cdot\frac{d\boldsymbol{P'}}{dt} < 0$. The first condition can be achieved if the mean $PM_{2.5}$ concentration decreases. The second condition occurs when $\frac{dc'_{i,j}}{dt} < 0$ in populous urban areas with $p'_{i,j} > 0$, whereas $\frac{dc'_{i,j}}{dt} > 0$ in rural areas with $p'_{i,j} < 0$. This condition can be achieved if the $PM_{2.5}$ concentration within populous urban areas reduces more than it does within rural areas. The third condition takes place when $\frac{dp'_{i,j}}{dt} < 0$ in polluted areas with $c'_{i,j} > 0$, whereas $\frac{dp'_{i,j}}{dt} > 0$ in clean areas with $c'_{i,j} < 0$. This condition can be achieved if city planning relocates people from living in polluted areas to clean areas. In summary, the variation in c_ρ can be decomposed into three parts, which are associated with the change in the mean $PM_{2.5}$ concentration, the spatial difference in $PM_{2.5}$ change and the demographic change, respectively.

References

1. Bo, Y.; Guo, C.; Lin, C.; Chang, L.; Chan, T.C.; Huang, B.; Lee, K.P.; Tam, T.; Lau, A.K.H.; Lao, X.Q.; et al. Dynamic Changes in Long-Term Exposure to Ambient Particulate Matter and Incidence of Hypertension in Adults. *Hypertension* **2019**, *74*, 669–677. [CrossRef] [PubMed]
2. Chan, T.C.; Zhang, Z.; Lin, B.C.; Lin, C.; Deng, H.B.; Chuang, Y.C.; Chan, J.W.M.; Jiang, W.K.; Tam, T.; Chang, L.; et al. Long-Term Exposure to Ambient Fine Particulate Matter and Chronic Kidney Disease: A Cohort Study. *Environ. Health Perspect.* **2018**, *126*, 107002. [CrossRef] [PubMed]
3. Guo, C.; Zhang, Z.; Lau, A.K.H.; Lin, C.Q.; Chuang, Y.C.; Chan, J.; Jiang, W.K.; Tam, T.; Yeoh, E.K.; Chan, T.C.; et al. Effect of long-term exposure to fine particulate matter on lung function decline and risk of chronic obstructive pulmonary disease in Taiwan: A longitudinal, cohort study. *Lancet Planet. Health* **2018**, *2*, e114–e125. [CrossRef]
4. Lao, X.Q.; Guo, C.; Chang, L.; Bo, Y.; Zhang, Z.; Chuang, Y.C.; Jiang, W.K.; Lin, C.; Tam, T.; Lau, A.K.H.; et al. Long-term exposure to ambient fine particulate matter (PM2.5) and incident type 2 diabetes: A longitudinal cohort study. *Diabetologia* **2019**, *62*, 759–769. [CrossRef] [PubMed]
5. Zhang, Z.; Chan, T.C.; Guo, C.; Chang, L.; Lin, C.; Chuang, Y.C.; Jiang, W.K.; Ho, K.F.; Tam, T.; Woo, K.S.; et al. Long-term exposure to ambient particulate matter (PM2.5) is associated with platelet counts in adults. *Environ. Pollut.* **2018**, *240*, 432–439. [CrossRef] [PubMed]
6. Apte, J.S.; Marshall, J.D.; Cohen, A.J.; Brauer, M. Addressing Global Mortality from Ambient PM2.5. *Environ. Sci. Technol.* **2015**, *49*, 8057–8066. [CrossRef] [PubMed]
7. Zhong, L.; Louie, P.K.K.; Zheng, J.; Yuan, Z.; Yue, D.; Ho, J.W.K.; Lau, A.K.H. Science–policy interplay: Air quality management in the Pearl River Delta region and Hong Kong. *Atmos. Environ.* **2013**, *76*, 3–10. [CrossRef]
8. Aunan, K.; Ma, Q.; Lund, M.T.; Wang, S. Population-weighted exposure to PM2.5 pollution in China: An integrated approach. *Environ. Int.* **2018**, *120*, 111–120. [CrossRef]
9. Brauer, M.; Amann, M.; Burnett, R.T.; Cohen, A.; Dentener, F.; Ezzati, M.; Henderson, S.B.; Krzyzanowski, M.; Martin, R.V.; Van Dingenen, R.; et al. Exposure Assessment for Estimation of the Global Burden of Disease Attributable to Outdoor Air Pollution. *Environ. Sci. Technol.* **2012**, *46*, 652–660. [CrossRef]
10. David, L.M.; Ravishankara, A.R.; Kodros, J.K.; Pierce, J.R.; Venkataraman, C.; Sadavarte, P. Premature Mortality Due to PM2.5 Over India: Effect of Atmospheric Transport and Anthropogenic Emissions. *GeoHealth* **2019**, *3*, 2–10. [CrossRef]
11. Van Donkelaar, A.; Martin, R.V.; Brauer, M.; Boys, B.L. Use of satellite observations for long-term exposure assessment of global concentrations of fine particulate matter. *Environ. Health Perspect.* **2015**, *123*, 135–143. [CrossRef] [PubMed]
12. Gui, K.; Che, H.; Wang, Y.; Wang, H.; Zhang, L.; Zhao, H.; Zheng, Y.; Sun, T.; Zhang, X. Satellite-derived PM2.5 concentration trends over Eastern China from 1998 to 2016: Relationships to emissions and meteorological parameters. *Environ. Pollut.* **2019**, *247*, 1125–1133. [CrossRef] [PubMed]
13. Li, J.; Zhu, Y.; Kelly, J.T.; Jang, C.J.; Wang, S.; Hanna, A.; Xing, J.; Lin, C.J.; Long, S.; Yu, L. Health benefit assessment of PM2.5 reduction in Pearl River Delta region of China using a model-monitor data fusion approach. *J. Environ. Manag.* **2019**, *233*, 489–498. [CrossRef] [PubMed]

14. Xue, T.; Zheng, Y.; Tong, D.; Zheng, B.; Li, X.; Zhu, T.; Zhang, Q. Spatiotemporal continuous estimates of PM2.5 concentrations in China, 2000–2016: A machine learning method with inputs from satellites, chemical transport model, and ground observations. *Environ. Int.* **2019**, *123*, 345–357. [CrossRef]
15. Zheng, H.; Zhao, B.; Wang, S.; Wang, T.; Ding, D.; Chang, X.; Liu, K.; Xing, J.; Dong, Z.; Aunan, K.; et al. Transition in source contributions of PM2.5 exposure and associated premature mortality in China during 2005–2015. *Environ. Int.* **2019**, *132*, 105111. [CrossRef]
16. Burnett, R.; Chen, H.; Szyszkowicz, M.; Fann, N.; Hubbell, B.; Pope, C.A.; Apte, J.S.; Brauer, M.; Cohen, A.; Weichenthal, S.; et al. Global estimates of mortality associated with long-term exposure to outdoor fine particulate matter. *Proc. Natl. Acad. Sci. USA* **2018**, *115*, 9592–9597. [CrossRef]
17. Lin, C.Q.; Li, Y.; Lau, A.K.H.; Deng, X.J.; Tse, K.T.; Fung, J.C.H.; Li, C.C.; Li, Z.Y.; Lu, X.C.; Zhang, X.G.; et al. Estimation of long-term population exposure to PM2.5 for dense urban areas using 1-km MODIS data. *Remote Sens. Environ.* **2016**, *179*, 13–22. [CrossRef]
18. Lu, Q.; Zheng, J.; Ye, S.; Shen, X.; Yuan, Z.; Yin, S. Emission trends and source characteristics of SO_2, NOx, PM10 and VOCs in the Pearl River Delta region from 2000 to 2009. *Atmos. Environ.* **2013**, *76*, 11–20. [CrossRef]
19. Ma, Z.; Hu, X.; Sayer, A.M.; Levy, R.; Zhang, Q.; Xue, Y.; Tong, S.; Bi, J.; Huang, L.; Liu, Y. Satellite-Based Spatiotemporal Trends in PM2.5 Concentrations: China, 2004–2013. *Environ. Health Perspect.* **2016**, *124*, 184–192. [CrossRef]
20. Lin, C.Q.; Li, Y.; Lau, A.K.H.; Li, C.C.; Fung, J.C.H. 15-Year PM2.5 Trends in the Pearl River Delta Region and Hong Kong from Satellite Observation. *Aerosol Air Qual. Res.* **2018**, *18*, 2355–2362. [CrossRef]
21. Lin, C.; Lau, A.K.H.; Lu, X.; Fung, J.C.H.; Li, Z.; Li, C.; Wong, A.H.S. Assessing Effect of Targeting Reduction of PM2.5 Concentration on Human Exposure and Health Burden in Hong Kong Using Satellite Observation. *Remote Sens.* **2018**, *10*, 2064. [CrossRef]
22. Lin, C.Q.; Lau, A.K.H.; Li, Y.; Fung, J.C.H.; Li, C.C.; Lu, X.C.; Li, Z.Y. Difference in PM2.5 variations between urban and rural areas over eastern China from 2001 to 2015. *Atmosphere* **2018**, *9*, 312. [CrossRef]
23. Wang, J.; Zhao, B.; Wang, S.; Yang, F.; Xing, J.; Morawska, L.; Ding, A.; Kulmala, M.; Kerminen, V.M.; Kujansuu, J.; et al. Particulate matter pollution over China and the effects of control policies. *Sci. Total Environ.* **2017**, *584–585*, 426–447. [CrossRef]
24. Lin, C.; Lau, A.K.H.; Fung, J.C.H.; Lao, X.Q.; Li, Y.; Li, C. Assessing the Effect of the Long-Term Variations in Aerosol Characteristics on Satellite Remote Sensing of PM2.5 Using an Observation-Based Model. *Environ. Sci. Technol.* **2019**, *53*, 2990–3000. [CrossRef] [PubMed]
25. Lin, C.Q.; Li, C.C.; Lau, A.K.H.; Yuan, Z.B.; Lu, X.C.; Tse, K.T.; Fung, J.C.H.; Li, Y.; Yao, T.; Su, L.; et al. Assessment of satellite-based aerosol optical depth using continuous lidar observation. *Atmos. Environ.* **2016**, *140*, 273–282. [CrossRef]
26. Li, Y.; Lin, C.; Lau, A.K.H.; Liao, C.; Zhang, Y.; Zeng, W.; Li, C.; Fung, J.C.H.; Tse, T.K.T. Assessing Long-Term Trend of Particulate Matter Pollution in the Pearl River Delta Region Using Satellite Remote Sensing. *Environ. Sci. Technol.* **2015**, *49*, 11670–11678. [CrossRef]
27. Li, C.; Lau, A.K.H.; Mao, J.; Chu, D.A. Retrieval, validation, and application of the 1-km aerosol optical depth from MODIS measurements over Hong Kong. *IEEE Trans. Geosci. Remote Sens.* **2005**, *43*, 2650–2658.
28. Lin, C.Q.; Li, Y.; Yuan, Z.B.; Lau, A.K.H.; Li, C.C.; Fung, J.C.H. Using satellite remote sensing data to estimate the high-resolution distribution of ground-level PM2.5. *Remote Sens. Environ.* **2015**, *156*, 117–128. [CrossRef]
29. Lin, C.Q.; Liu, G.; Lau, A.K.H.; Li, Y.; Li, C.C.; Fung, J.C.H.; Lao, X.Q. High-resolution satellite remote sensing of provincial PM2.5 trends in China from 2001 to 2015. *Atmos. Environ.* **2018**, *180*, 110–116. [CrossRef]
30. Geng, G.; Zhang, Q.; Martin, R.V.; van Donkelaar, A.; Huo, H.; Che, H.; Lin, J.; He, K. Estimating long-term PM2.5 concentrations in China using satellite-based aerosol optical depth and a chemical transport model. *Remote Sens. Environ.* **2015**, *166*, 262–270. [CrossRef]
31. Peng, J.; Chen, S.; Lü, H.; Liu, Y.; Wu, J. Spatiotemporal patterns of remotely sensed PM2.5 concentration in China from 1999 to 2011. *Remote Sens. Environ.* **2016**, *174*, 109–121. [CrossRef]
32. Van Donkelaar, A.; Martin, R.V.; Brauer, M.; Kahn, R.; Levy, R.; Verduzco, C.; Villeneuve, P.J. Global estimates of ambient fine particulate matter concentrations from satellite-based aerosol optical depth: Development and application. *Environ. Health Perspect.* **2010**, *118*, 847–855. [CrossRef] [PubMed]
33. OECD. *Redefining "Urban": A New Way to Measure Metropolitan Areas*; OECD Publishing: Paris, France, 2012.
34. Li, Z.; Wen, Q.; Zhang, R. Sources, health effects and control strategies of indoor fine particulate matter (PM2.5): A review. *Sci. Total Environ.* **2017**, *586*, 610–622. [CrossRef] [PubMed]

35. Li, Z.; Che, W.; Lau, A.K.H.; Fung, J.C.H.; Lin, C.; Lu, X. A feasible experimental framework for field calibration of portable light-scattering aerosol monitors: Case of TSI DustTrak. *Environ. Pollut.* **2019**, *255*, 113136. [CrossRef] [PubMed]
36. Li, Z.; Che, W.; Frey, H.C.; Lau, A.K.H.; Lin, C. Characterization of PM2.5 exposure concentration in transport microenvironments using portable monitors. *Environ. Pollut.* **2017**, *228*, 433–442. [CrossRef]
37. Li, Y.; Lau, A.K.H.; Fung, J.C.H.; Ma, H.; Tse, Y. Systematic evaluation of ozone control policies using an Ozone Source Apportionment method. *Atmos. Environ.* **2013**, *76*, 136–146. [CrossRef]
38. Lu, X.; Yao, T.; Li, Y.; Fung, J.C.H.; Lau, A.K.H. Source apportionment and health effect of NOx over the Pearl River Delta region in southern China. *Environ. Pollut.* **2016**, *212*, 135–146. [CrossRef]
39. Wang, X.; Liu, H.; Pang, J.; Carmichael, G.; He, K.; Fan, Q.; Zhong, L.; Wu, Z.; Zhang, J. Reductions in sulfur pollution in the Pearl River Delta region, China: Assessing the effectiveness of emission controls. *Atmos. Environ.* **2013**, *76*, 113–124. [CrossRef]